# The Effect of 2D Van der Waals Materials on the Photoresponse of Upconversion Nanoparticles

Hangshuai Jin[1], Zhimin Zhang[1], Zhefei Zhang[2], Pit On Chim[2], Lei Liu[1*] and Mingdong Dong[2*]

[1]*Institute for Advanced Materials, Jiangsu University, China*
[2]*Interdisciplinary Nanoscience Center (iNANO), Aarhus University, 8000 Aarhus C, Denmark*
*E-mail: liul@ujs.edu.cn; dong@inano.au.dk*
**Corresponding Authors*

Received 17 May 2019; Accepted 13 June 2019;
Publication 22 January 2020

## Abstract

Upconversion materials, a type of novel functional materials, have many good physicochemical properties, such as high luminescence stability, high chemical stability, long luminous life, and low potential biotoxicity. How to regulate the luminescence of upconversion materials is a significant challenge. Two-dimensional (2D) Van der Waals materials are a new type of nanomaterials with a layer structure. Some of them are capable of quenching the luminescence of dyes, which could be applied in the modulation of optical response of upconversion materials. Therefore, in this work, we explored the photoresponse of $\beta$-$NaYF_4$:Yb/Er triggered by 2D Van der Waals materials including graphene oxide, $MoS_2$, g-$C_3N_4$ and BN. The results obtained in this work would be beneficial for the further application of luminescence modulation of UCNPs. Using UCNPs as a potential fingerprint of 2D Van der Waals materials, their optical response might be used to distinguish the 2D Van der Waals materials.

**Keywords:** Optical response, $\beta$-$NaYF_4$:Yb/Er, GO, g-$C_3N_4$, $MoS_2$, BN.

*Journal of Self-Assembly and Molecular Electronics, Vol. 7_1,* 73–86.
doi: 10.13052/jsame2245-4551.7.004

## 1 Introduction

Upconversion materials has been widely concerned due to good physicochemical properties since they were proposed by Auzel, Ovsyankin and Feofilov [1] in the 1960s. A lot of attention was paid to the study of upconversion materials to optimize their efficiency or expand their range of applications. By the end of the 20th century, the upconversion materials have a wide range of applications in various fields due to their unique characteristics, especially in biomedical field.

Upconversion materials with many good physicochemical properties are considered as a type of novel functional material, such as high luminescence stability, high chemical stability [2], long luminous life [3, 4], and low potential biotoxicity [5, 6]. In addition, they could absorb near-infrared light which has low damage to biological tissue, deep penetration of tissue, and no biological background fluorescence interference. Accordingly, they could be applied in biomedical field, e.g. photodynamic therapy [7, 8], biomolecular detection [9, 10], bioimaging [11–14], biosensing [15, 16] and drug delivery [17–19], etc. Qian Liu [20] has reported that $Gd^{3+}$, $Yb^{3+}$, and $Er^{3+}$ doped $NaLuF_4$ could be used for bioimaging in mice. In order to control the drug release by pH, functional upconversion nanoparticles ($NaYF_4$:Yb/Er) were constructed by modifying with polyethylene glycol (PEG) and loading doxorubicin [21].

As is known to all, the upconversion material is a luminescent material that absorbs long wavelength light and emits short wavelength light, which is anti-Stockes effect. Achieving the recurrence/absence/appearance/enhancement of upcoversion fluorescence through the principle of energy transfer could be well used in the field of biosensing. The modulation of photoresponse of upconversion materials is the essence in the application of biosensing. How to regulate the luminescence of upconversion materials is a significant challenge. Two-dimensional (2D) Van der Waals materials are a new type of nanomaterials with a lamellar structure, which have a horizontal dimension of more than 100 nm, but only a single or a few atom layer thickness (typically less than 5 nm). The excellent conductivity along the 2D basal plane facilitate the transport performance of photogenerated electron or hole which is a key role in photoresponse field [22–24]. Some 2D Van der Waals materials can quench the luminescence of dyes, such as graphene and molybdenum disulfide, which could be applied in the modulation of optical response of upconversion materials. Combining the 2D Van der Waals materials with upconversion materials can not only

bring new fundamental investigation, but also extend the application of upconversion materials.

Herein, we mainly use different 2D Van der Waals materials with unique physical properties to explore the modulation effect of 2D Van der Waals materials on the photoresponse of upconversion nanoparticles (UCNPs). Firstly, the UCNPs $\beta$-$NaYF_4$:Yb/Er were prepared by thermal solvent method. The photoresponse of $\beta$-$NaYF_4$:Yb/Er triggered by two-dimensional Van der Waals materials including GO, $MoS_2$, g-$C_3N_4$ and BN was systematically investigated. The quenching and enhancing effect on the luminescence of UCNPs by different 2D Van der Waals materials was revealed. GO, $MoS_2$ can quench and g-$C_3N_4$ can enhance the luminescence of UCNPs while BN has no effect. The results obtained in this work would contribute to the further application of luminescence modulation of UCNPs. The optical response of UCNPs as a potential fingerprint of 2D Van der Waals materials might also be used to distinguish the 2D Van der Waals materials.

## 2 Experimental Materials and Methods

### 2.1 Materials

Graphene oxide (GO) (50–200 nm), $MoS_2$ (20–500 nm) and g-$C_3N_4$ were purchased from Nanjing Xianfeng Nanomaterials Co., Ltd. $Y_2O_3$, $Yb_2O_3$, $Er_2O_3$, NaOH, $NH_4F$, and BN were obtained from Aladdin Ltd. Deionized water was applied to all solution preparations.

### 2.2 The Preparation of $\beta$-$NaYF_4$:Yb/Er

Based on the previous literature reports [25], we optimized the experimental protocol to synthesize upconverting nanoparticles ($NaYF_4$:Yb/Er). Firstly, 0.4 mmol $Y_2O_3$, 0.09 mmol $Yb_2O_3$ and 0.01 mmol $Er_2O_3$ were placed into a 100 mL beaker, then excess of diluted hydrochloric acid was added until the solution was colorless and transparent. Subsequently, the obtained solution was dried on an electric heating jacket, 1 mmol (Y: Yb: Er = 80: 18: 2) rare earth chloride ($LnCl_3$) solid was obtained. The obtained solid was transferred to a 100 mL three-necked flask, and 12 mL of oleic acid (OA) and 15 mL of 1-octadecene (ODE) were added into the three-necked flask. The mixture was heated to 120°C to dissolve until the solid disappeared completely, and a bright yellow solution was obtained. After naturally cooling to room temperature, 10 mL of methanol with 5 mmol sodium hydroxide (NaOH) and 8 mmol ammonium fluoride ($NH_4F$) was added slowly. After reacting

for about 30 min, it was heated to 60°C for 20 min to remove methanol from the solution, and then heated to 100°C for 20 min to remove water and oxygen, then heated to 310°C and maintained under nitrogen for 1 h. After naturally cooling to room temperature, the product was precipitated by adding ethanol. Subsequently, centrifugation was carried out at a rotational speed of 8000 rpm. Finally, the oleic acid-coated upconversion nanoparticles were obtained after washed about 3–4 times with a mixture of water and ethanol (v:v=1:1). The obtained product was divided into two parts. One part was dispersed in water/cyclohexane, and the other part was dried in a vacuum drying oven at 60°C.

### 2.3 The Characterization of UCNPs and UCNPs/2D Materials

TEM: The prepared samples were formulated into a low-concentration aqueous solution, which was dropped on a 100-mesh copper net by a pipette, and allowed to stand for 10 min. The excess liquid was removed, and the copper net was naturally air-dried. Finally, the morphology was characterized by transmission electron microscopy (Tecnai 12).

SEM: The prepared samples were formulated into a low-concentration aqueous solution, which was then dropped on a silicon wafer by a pipette, standing for 10 min. The excess liquid was removed, and the silicon wafer was naturally air-dried. It was then placed on an SEM sample stage with conductive paste; the morphology was characterized by field emission scanning electron microscopy (JSM-7001F). Acceleration voltage: 15 kV.

AFM: The prepared samples (about 10 $\mu$L) were dropped onto the surface of fresh mica and deposited for 10 minutes to remove the liquid. In the MultiMode VIII SPM (Bruker), all AFM images were recorded by tapping mode, using silicon cantilever probe (OMCL AC160TS-R3; Olympus) with a spring constant of 26 $\mathrm{Nm}^{-1}$. AFM images were done with a scan frequency of 1 Hz and a resolution of $512 \times 512$.

Raman spectroscopy: The prepared samples were all deposited as powder on a glass slide, and then excited by a Raman spectrometer DXR at 514.5 nm to detect the Raman spectrum of the sample. Wave range: 500–3500 $\mathrm{cm}^{-1}$.

### 2.4 Luminescence of $\beta$-$NaYF_4$:Yb/Er Triggered by 2D Van der Waals Materials

Preparing several equal concentrations of $\beta$-$NaYF_4$:Yb/Er aqueous solution, add different volumes of 2D Van der Waals materials aqueous

solution to form a mixture of two-dimensional Van der Waals materials and $\beta$-$NaYF_4$:Yb/Er with concentration gradient, and then perform upconversion fluorescence detection. The light source with 980 nm laser was used, and the fluorescence intensity was detected using a fluorescence spectrophotometer.

## 3 Results and Discussion

The upconversion nanoparticles $NaYF_4$:Yb/Er synthesized by thermal solvent method were characterized by TEM and SEM, as shown in Figures 1a and 1b respectively. The morphology of $\beta$-$NaYF_4$:Yb/Er was presented to be particles with a size of $45.9 \pm 0.3$ nm (Figure 1c). The structure of $\beta$-$NaYF_4$:Yb/Er is hexagonal phase ($\beta$) as shown in Figure 1d.

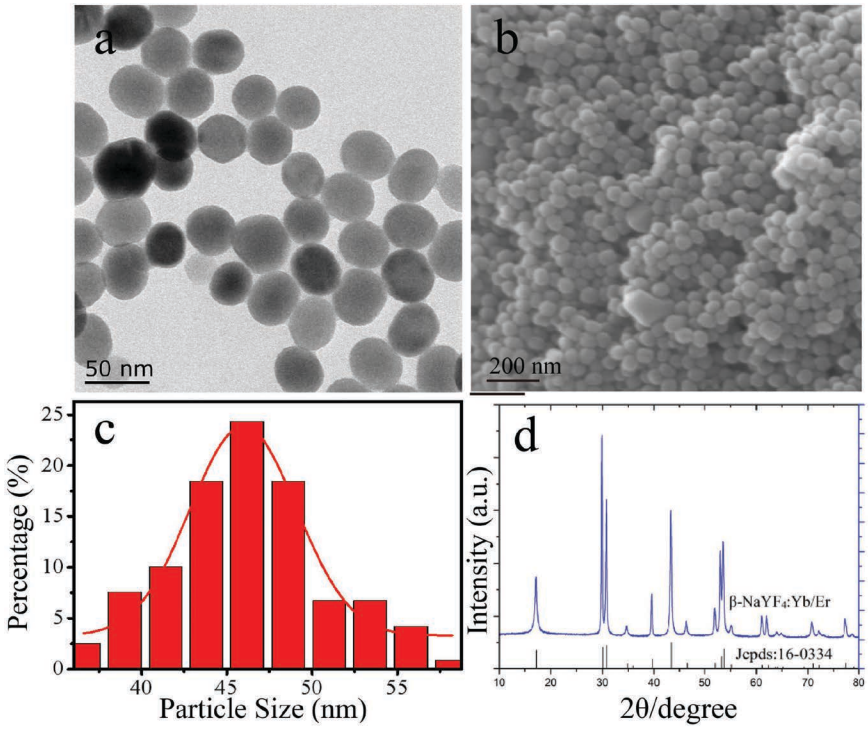


**Figure 1** The morphology of $\beta$-$NaYF_4$: Yb/Er nanoparticles. (a) TEM image, (b) SEM image, and (c) size distribution collected from TEM, (d) XRD.

### 3.1 Optical Response of $\beta$-$NaYF_4$:Yb/Er Triggered by GO

Graphene oxide (GO) is a single-layer 2D Van der Waals material with good physical and chemical properties. As characterized by AFM and TEM, it displays a lamellar structure with the height of 1.1 nm (Figures 2a–2c). Raman spectroscopy was used to detect the typical feature of GO, with D band at 1356 $cm^{-1}$ and G band at 1601 $cm^{-1}$. The value of ID/IG is related to the defects and vacancies of GO (Figure 2d). Subsequently, we investigated the photoresponse of $\beta$-$NaYF_4$:Yb/Er triggered by GO.

The optical response between $\beta$-$NaYF_4$:Yb/Er and GO at different concentrations (0–100 $\mu$g/mL) was measured by a Fluorescence spectrophotometer and near infrared laser with 980 nm. The result is presented in Figure 3. GO with different concentrations presented the quenching effect on the $\beta$-$NaYF_4$:Yb/Er which reflected by the decrement of fluorescence intensity of $\beta$-$NaYF_4$:Yb/Er with 407 nm, 524 nm

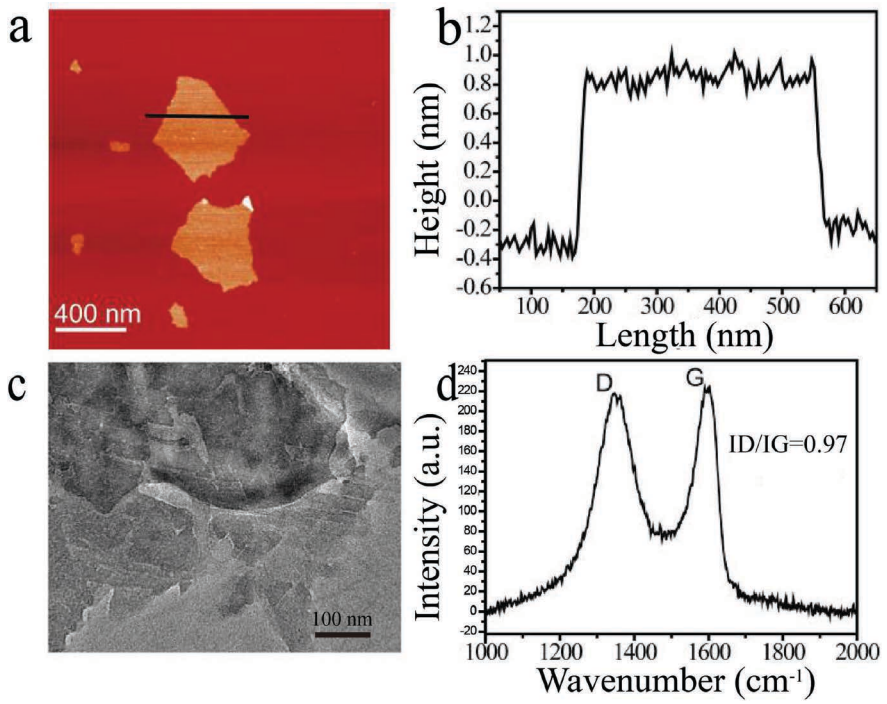


**Figure 2** The morphology and Raman spectra of GO. (a) AFM height image of GO, (b) the height profile along the black line in (a), (c) the TEM image of GO and (d) The Raman spectrum of GO.

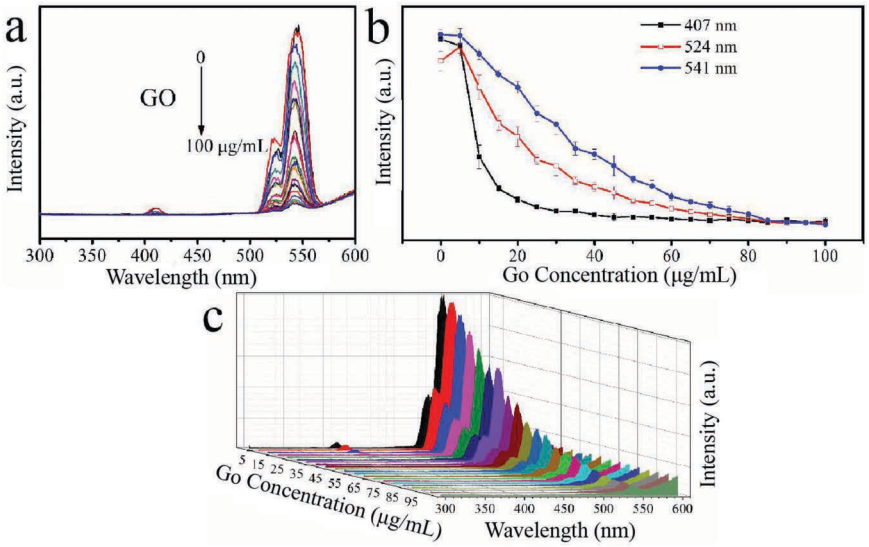


**Figure 3** The quench effect of GO concentration on the upconversion luminescence (UCL) of $\beta$-$NaYF_4$:Yb/Er (a) and UCL intensity change vs. GO concentration according to different peaks at 407 nm (black line), 524 nm (red line) and 541 nm (blue line) (b, different Y axis) and 3D image of UCL (c).

and 541 nm. When GO concentration is 10 $\mu$g/mL, the quenching rate of $\beta$-$NaYF_4$:Yb/Er reaches 50.18% at 407 nm, while it is 14.61% and 9.5% at 524 and 541 nm, respectively. With increasing GO concentration to 25 $\mu$g/mL, the quenching effect displayed maximum at 407 nm, but at 524 and 540 nm, it is saturated with the concentration of GO at 85 $\mu$g/mL.

The hybrids formation of $\beta$-$NaYF_4$:Yb/Er and GO facilitate the optical quench of $\beta$-$NaYF_4$:Yb/Er. The complex structure was characterized as shown in Figure 4. When GO interacts with $\beta$-$NaYF_4$:Yb/Er, a large number of $\beta$-$NaYF_4$:Yb/Er particles adhere to the surface of GO and then quench the fluorescence of $\beta$-$NaYF_4$:Yb/Er by electron transfer.

### 3.2 Optical Response of $\beta$-$NaYF_4$:Yb/Er Triggered by $MoS_2$, g-$C_3N_4$ and BN

The basic morphologies of $MoS_2$, g-$C_3N_4$ and BN, were characterized (Figure 5a–d and S1). The optical response of upconversion nanoparticles treated by different concentrations of $MoS_2$, g-$C_3N_4$ and BN was measured

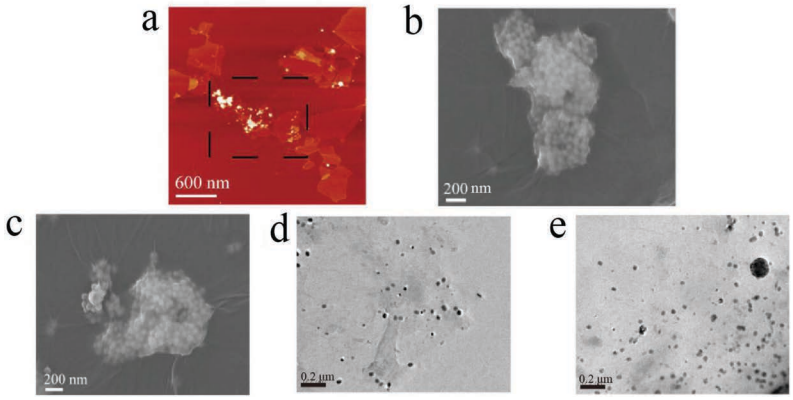


**Figure 4** The morphology of hybrids of $\beta$-$NaYF_4$:Yb/Er and GO. (a) The AFM height image, (b) and (c) SEM images, (d) and (e) TEM images. The dash line in (a) indicate the part where Go and UCNPs are combined together.

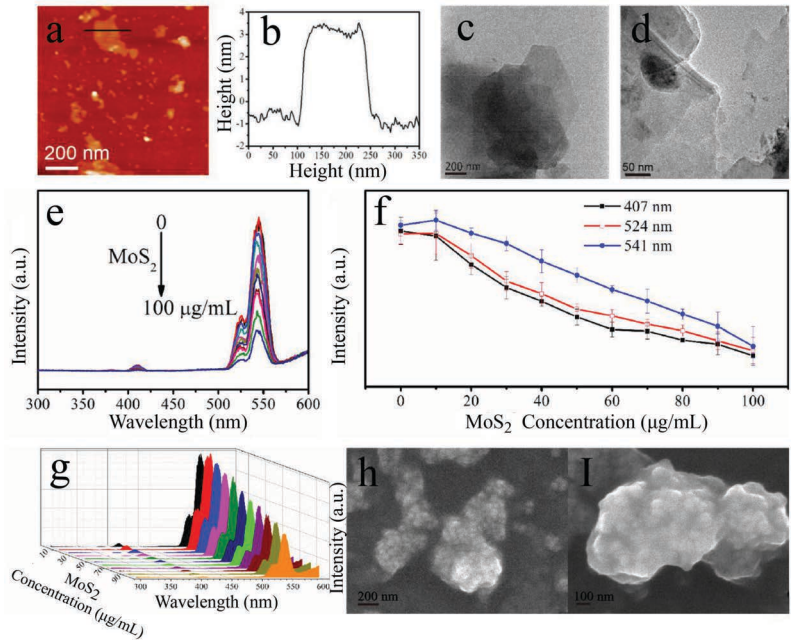


**Figure 5** AFM (a) and corresponding height map (b) and TEM map (c, d) of $MoS_2$. UCL of $\beta$-$NaYF_4$:Yb/Er triggered by $MoS_2$ with different concentrations (e) and UCL intensity change vs. $MoS_2$ concentration according to different peaks at 407 nm (black line), 524 nm (red line) and 541 nm (blue line) (f, different Y axis) and 3D image of UCL (g). h,I: SEM images of the hybrids of $\beta$-$NaYF_4$:Yb/Er and $MoS_2$.

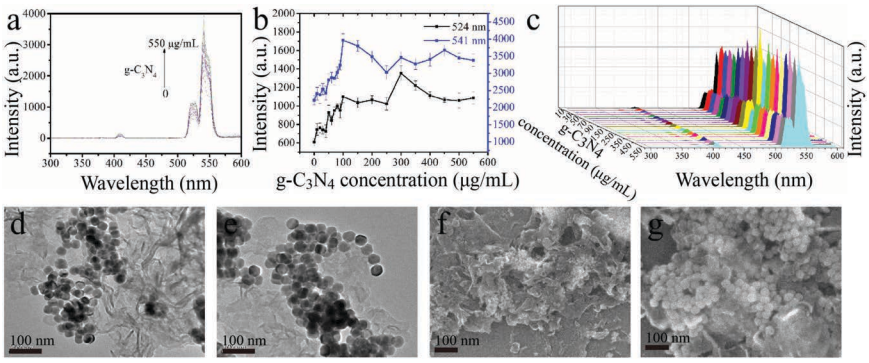


**Figure 6** UCL of $\beta$-$NaYF_4$:Yb/Er triggered by g-$C_3N_4$ with different concentrations (a) and corresponding intensity change trend chart of the up-conversion emissions peaked at 524 nm and 541 nm (b, different Y axis) and 3D image of UCL (c); d-g: TEM (d, e) and SEM (f, g) images of the hybrids of g-$C_3N_4$ with $\beta$-$NaYF_4$:Yb/Er.

as shown in Figures 5–7. In the case of $MoS_2$, it presented the quenching effect on the luminescence of $\beta$-$NaYF_4$:Yb/Er at 407 nm, 524 nm and 541 nm, which displayed the stronger effect with the increment of concentration of $MoS_2$ (0–100 $\mu$g/mL) (Figure 5). The quenching effect of $MoS_2$ on $\beta$-$NaYF_4$:Yb/Er conforms to a certain linear relationship. When $MoS_2$ concentration reaches 100 $\mu$g/mL, the quenching effect is still increasing. However, compared to GO, the quenching efficiency of $MoS_2$ is lower than that of GO. The mechanism is due to the interaction between the nanoparticles of $\beta$-$NaYF_4$:Yb/Er and $MoS_2$. The attachment of $\beta$-$NaYF_4$:Yb/Er onto $MoS_2$ or the encapsulation in $MoS_2$ possibly results in energy transfer and fluorescence quenching of $\beta$-$NaYF_4$:Yb/Er in Figures 5h and 5i.

The optical response of $\beta$-$NaYF_4$:Yb/Er triggered by g-$C_3N_4$ and BN was investigated as well (Figures 6 and 7) no quenching effect on the luminescence of $\beta$-$NaYF_4$:Yb/Er was obtained for the g-$C_3N_4$, but a certain enhancement to a certain extent was detected, which indicates that there might be no electron transfer from $\beta$-$NaYF_4$:Yb/Er to g-$C_3N_4$. On the contrary, some electron might transfer to $\beta$-$NaYF_4$:Yb/Er from g-$C_3N_4$. The g-$C_3N_4$ and $\beta$-$NaYF_4$:Yb/Er do interact with each other in a way which makes them combine with each other, as shown in Figures 6d–g. However, in the case of BN, no any quenching and enhancing effect on the luminescence of $\beta$-$NaYF_4$:Yb/Er (Figures 7a–c) were observed, mainly due to the weak interaction between the BN and $\beta$-$NaYF_4$:Yb/Er (Figures 7d–g) and also possible due to similar energy level of electron staying in BN and UCNPs.

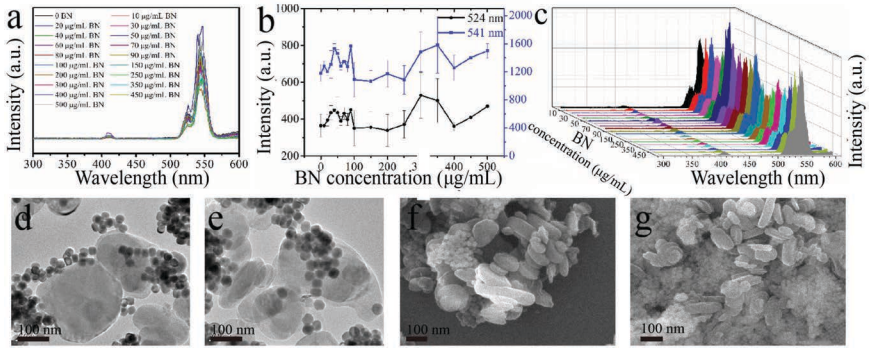


**Figure 7** UCL of $\beta$-$NaYF_4$:Yb/Er triggered by BN with different concentrations (a) and corresponding intensity change trend chart of the up-conversion emissions peaked at 524 nm and 541 nm (b, different Y axis) and 3D image of UCL (c); d–g: TEM (d, e) and SEM (f, g) images of the hybrids of BN with $\beta$-$NaYF_4$:Yb/Er.

## 4 Conclusion

In this work, the photoresponse of $\beta$-$NaYF_4$:Yb/Er treated by four different 2D Van der Waals materials, including GO, $MoS_2$, g-$C_3N_4$ and BN was investigated, which presented distinct effects on the luminescence of UCNPs. Both GO and $MoS_2$ could quench the luminescence of UCNPs, in which GO exhibited a stronger ability than $MoS_2$. However, in the case of g-$C_3N_4$, the enhancing effect on the luminescence was observed, which might be due to the opposite electron transfer between the 2D Van der Waals material and UCNPs. BN could not display any effect due to the weak interaction between BN and $\beta$-$NaYF_4$:Yb/Er and also possible due to similar energy level of electron staying in BN and UCNPs. The data obtained above would shed light on the further application of luminescence regulation of UCNPs. Using UCNPs as a potential fingerprint of 2D Van der Waals materials, their optical response might be used to distinguish the 2D Van der Waals materials.

## Acknowledgments

This work was financially supported by the National Natural Science Foundation of China (21573097, 51503087).

## References

[1] A. Francois, Cheminform, **35**, 139–173 (2004).

[2] M. X. Yu, F. Y. Li, Z. G. Chen, H. He, Z. Cheng, Y. Hong, Anal. Chem, **81**, 930–935 (2009).
[3] Y. I. Park, K. T. Lee, Y. D. Suh, Chem. Soc. Rev, **44**, 1302–1317 (2015).
[4] J. Zhou, Z. Liu, F. Y. Li, Chem. Soc. Rev, **41**, 1323–1349 (2012).
[5] Y. M. Yang, F. Liu, X. G. Liu, B. G. Xing, Nanoscale, **5**, 231–238 (2013).
[6] W. Wei, T. C. He, X. Teng, S. Wu, M. Lin, Z. Hua, Small, **8**, 2271–2276 (2012).
[7] J. Xu, L. Xu, C. Wang, R. Yang, Q. Zhuang, X. Han, Acs Nano, **11**, 4463–4474 (2017).
[8] D. Wang, L. Zhu, Y. Pu, J. X. Wang, J. F. Chen, L. Dai, Nanoscale, **9**, 11214–11221 (2017).
[9] R. R. Deng, X. J. Xie, V. Marc, C. Young-Tae, X. G. Liu, J. Am Chem Soc, **133**, 20168–20171 (2011).
[10] H. Li, L. Shi, D. E. Sun, P. Li, Z. Liu, Biosens Bioelectron, **86**, 791–798 (2016).
[11] X. Wu, Y. Zhang, K. Takle, O. Bilsel, Z. Li, H. Lee, Z. Zhang, D. Li, Acs Nano, **10**, 1060–1066 (2016).
[12] J. Xu, P. Yang, M. Sun, H. Bi, B. Liu, D. Yang, S. Gai, Acs Nano, **11**, 4133–4144 (2017).
[13] H. Bi, Y. Dai, P. Yang, J. Xu, D. Yang, S. Gai, F. He, B. Liu, Small, **14**, 1703809 (2018).
[14] S. F. Lim, R. Riehn, W. S. Ryu, N. Khanarian, C. K. Khanarian, D. Khanarian, R. H. Khanarian, Nano Lett, **6**, 169–174 (2006).
[15] F. Zhang, L. Liu, S. Wang, B. Zhao, P. Pei, Y. Fan, X. Li, Angew. Chem. Int. Ed. Engl, **57**, 7518–7522 (2018).
[16] S. Yang, Z. Lin, L. Kong, X. Yao, X. Y. Liu, Adv. Funct. Mater, **27**, 1700628–1700638 (2017).
[17] G. Tian, Z. J. Gu, L. J. Zhou, Y. Wenyan, Adv Mater, **24**, 1226–1231 (2012).
[18] S. Han, A. Samanta, X. Xie, L. Huang, J. Peng, S. J. Park, D. B. Teh, Y. Choi, Y. T. Chang, Adv Mater, **29**, 1700244–1700251 (2017).
[19] L. Bei, Y. Chen, C. Li, H. Fei, Z. Hou, S. Huang, H. Zhu, X. Chen, J. Lin, Adv. Funct. Mater, **25**, 4717–4729 (2015).
[20] Q. Liu, Y. Sun, T. Yang, J Am Chem Soc, **133**, 17122–17125 (2011).
[21] C. Wang, L. Cheng, Z. Liu, Biomaterials, **32**, 1110–1120 (2011).
[22] Z. Wang, H. Wu, Q. Li, Nanoscale, **10**, 18178–18185 (2018).
[23] Z. Wang, Q. Li, Y. Chen, NPG Asia Mater, **10**, 702–713 (2018).
[24] P. Zhang, Z. Wang, L. Liu, Appl. Mater. Mater, **14**, 151–158 (2019).
[25] L. Xia, X. Kong, X. Liu, Biomaterials, **35**, 4146–4156 (2014).

## Biographies

**Hangshuai Jin** obtained the bachelor degree in Material Processing and Control Engineering at Quzhou College (Zhejiang, China). Hangshuai Jin is now a mater student of School of Materials Science and Engineering in Jiangsu University (JiangSu, China), The research interest focuses on the study of antimicrobial mechanism by using AFM.

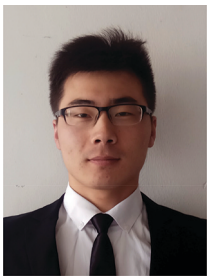

**Zhimin Zhang** was born in 1992, and he graduated from Anhui University of Technology in 2016 majoring in Polymer Materials and Engineering. At present, he is studying Master of Materials science and engineering in Jiangsu University.

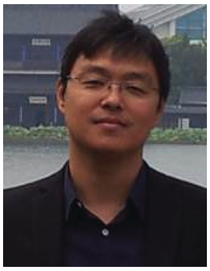

**Lei Liu** has completed his Ph.D in 2010 from National Center for Nanoscience and Technology, China, after that he went to iNANO Center of Aarhus University, Denmark for postdoctoral studies about 3 years working with Prof. Flemming Besenbacher and Dr, Mingdong Dong. He became the Young Distinguish Professor of Jiangsu University China, in 2013. Since 2014, he has been the research and Jiangsu Specially-Appointed Professor of China. His research interest focuses on the scanning probe microscopy, characterization of nanomaterials.

**Mingdong Dong** achieved Ph.D. in 2006 in Department of Physics and Astronomy, then he continue his postdoc study at Rowland Institute, Harvard University. Since 2009, he worked as an associate professor in Bio-SPM group, Interdisciplinary Nanoscience Center, Aarhus University (Denmark). Mingdong Dong long-term commits to the development and application of scanning probe microscopy techniques. He successfully expanded biomolecular imaging application in a liquid phase with high resolution. He developed for the first time the use of force microscopy microsecond. His interests focus on the structure of the material and research functions.